



## Desulfurization of air at high and low H<sub>2</sub>S concentrations

Yehya Elsayed<sup>a</sup>, Mykola Seredych<sup>b</sup>, Andrew Dallas<sup>a</sup>, Teresa J. Bandosz<sup>b,\*</sup>

<sup>a</sup> Corporate Technology, Donaldson Company Inc., Minneapolis, MN 55431, United States

<sup>b</sup> Department of Chemistry, The City College of the City University of New York, 138th Street and Convent Ave, New York, NY 10031, United States

### ARTICLE INFO

#### Article history:

Received 5 May 2009

Received in revised form 10 August 2009

Accepted 11 August 2009

#### Keywords:

Activated carbons  
H<sub>2</sub>S adsorption  
Surface chemistry  
Pore structure  
Reactive adsorption

### ABSTRACT

Several commercially available coconut-based activated carbons were tested as adsorbents of hydrogen sulfide (H<sub>2</sub>S) at high and low H<sub>2</sub>S concentrations. These carbons were compared to an experimental coconut-based carbon modified by impregnation with strongly basic compounds and an oxidant. The breakthrough curves for H<sub>2</sub>S at 3000 ppm and 10 ppm were measured at room temperature. The effects of humidity and water content on H<sub>2</sub>S removal were investigated. The carbon samples were characterized before and after H<sub>2</sub>S adsorption using XRF, sorption of nitrogen, thermal analysis in combination with mass spectrometry (TGA–MS) and thermal desorption–gas chromatography–mass spectrometry (TD–GC–MS), along with pH measurements. These methods were used to track the activated carbon surface chemical changes upon H<sub>2</sub>S adsorption/reactive adsorption. The amount of H<sub>2</sub>S adsorbed on all activated carbons was found to be dependent on the amount of surface basic groups. TGA–MS and TD–GC–MS analysis revealed H<sub>2</sub>S is adsorbed via reactive adsorption mechanisms. Metal sulfates, elemental sulfur, carbon sulfide, oxides of sulfur and dihydrogen disulfide are the products of surface reactions.

© 2009 Elsevier B.V. All rights reserved.

### 1. Introduction

Controlling hydrogen sulfide (H<sub>2</sub>S) concentrations is critical in many applications due to it being one of the most malodorous compounds [1,2]. The characteristic odor of H<sub>2</sub>S is detected at a threshold of 0.0047 ppm. Hydrogen sulfide is reported to be toxic, harmful to human health, has damaging effects on many industrial catalysts, and is known to be a major source of acid rain when oxidized in the atmosphere [1,2]. H<sub>2</sub>S becomes harmful to human health when inhaled and can be deadly depending on the exposure concentration and a duration of the exposure. Eye irritation starts to occur around 10–20 ppm. The risk of pulmonary edema is noticeable above 300 ppm. Exposure to concentrations over 1000 ppm might lead to death [3]. H<sub>2</sub>S can be removed from air streams using several filtration techniques involving biological approaches including biofilters and biotrickling filters [4–7], adsorption [8–14] or catalytic oxidations [2,15–17]. The later seems to be the most promising due to its efficiency in converting H<sub>2</sub>S without the formation of any undesired byproducts [10,12,16,17]. Even though, most of the commercially available non-impregnated activated carbons are not efficient at removing H<sub>2</sub>S owing to the nonspecificity of their surface [9], catalytically active carbon is

currently one of the most used solid adsorbents for H<sub>2</sub>S conversion in the presence of water vapor. The surface chemistry of activated carbons can be modified to introduce specific chemical groups to selectively target H<sub>2</sub>S retention. Several chemical modifications [2,8–18] of activated carbon are commonly used to enhance the performance for H<sub>2</sub>S removal, including: impregnation with sodium and potassium hydroxide; sodium and potassium carbonate or bicarbonate; potassium phosphate; or other chemicals such as magnesium oxide (MgO), potassium iodide (KI), and potassium permanganate (KMnO<sub>4</sub>). Mixtures of these chemicals are sometimes used.

Most of the H<sub>2</sub>S adsorption testing reported in the literature has been performed at high concentrations (>500 ppm) in order to minimize a test time and the resources required [11–18]. Although accelerated testing has several economic advantages, it may provide misleading results for choosing the best performing adsorbent for low concentration applications. This is because it is known that the adsorption mechanism can vary significantly with concentration when surface features are involved [11–18]. As the contaminant concentration increases the reaction mechanism can change depending on the availability of the centers and the energy of interactions. Hence, for any adsorption study it is important to evaluate adsorbent surface chemistry, surface–contaminant interactions, and structural features. Moreover, it is necessary to understand both the equilibrium capacity and kinetic limitations of a specific contaminant's adsorption. Such understanding plays a

\* Corresponding author. Tel.: +1 212 650 6017; fax: +1 212 650 6107.  
E-mail address: [tbandosz@ccny.cuny.edu](mailto:tbandosz@ccny.cuny.edu) (T.J. Bandosz).

critical role in choosing the best activated carbon for designing the most efficient chemical filter. For  $H_2S$  removal, the chosen adsorbent must strike a balance between its high and low concentration capacity and the kinetics of adsorption.

The objective of this work is to evaluate the performance of several commercially available activated carbons for  $H_2S$  removal at both low and high concentrations. The study focuses on analyzing the differences in the  $H_2S$  adsorption under different experimental conditions. This includes the effect of impregnation, water content and humidity on the catalytic performance of activated carbon for  $H_2S$  oxidation. The samples were characterized before and after  $H_2S$  adsorption to define the nature of the products deposited on the exhausted materials and thus to better understand the mechanism of reactive adsorption.

## 2. Experimental

### 2.1. Materials

Four activated carbons were used for the study of  $H_2S$  adsorption. They are referred to as C-1, C-2, C-3, and C-4. The first three are coconut-based non-impregnated activated carbons with surface pH in the basic region and they are applied in industry as  $H_2S$  adsorbents. Sample C-4 is a modified activated carbon with a combination of impregnants to enhance its surface affinity for  $H_2S$  removal via specific adsorption and catalytic oxidation. One of the impregnants on this carbon is strongly basic in its chemical nature and the other is classified as an oxidant. The carbons were chosen owing to their alkaline surface and structural differences and to their satisfactory initial performance in the screening test done at low  $H_2S$  concentration for a wider spectrum of activated carbons available on the market (in total 11 carbons were tested).

### 2.2. Methods

#### 2.2.1. Boehm titration

The amount of oxygenated surface groups was determined using the Boehm titration method [19,20]. The details of the experimental procedure are described in [Supplementary Information](#).

#### 2.2.2. pH

The pH of a carbon sample suspension provides information about the overall acidity and basicity of the surface. A sample of 0.4 g of dry carbon powder was added to 20 ml of water and the suspension was stirred overnight to reach equilibrium. Then the pH of suspension was measured.

#### 2.2.3. Sorption of nitrogen

Nitrogen isotherms were measured using an ASAP 2010 (Micromeritics) at 77 K. The details of the experimental procedure are described in [Supplementary Information](#).

The isotherms were used to calculate the BET surface area,  $S_{BET}$ , micropore volume,  $V_{mic}$ , mesopore volume,  $V_{meso}$  and total pore volume,  $V_t$ . The pore volumes and pore size distributions were calculated using Density Functional Theory (DFT) [21,22].

#### 2.2.4. Water isotherm

Measurement of the water isotherm was performed using a VTI model SGA-100 Vapor Sorption Analyzer. The details of the experimental procedure are described in [Supplementary Information](#).

#### 2.2.5. Breakthrough testing

**2.2.5.1. Evaluation of  $H_2S$  sorption capacity (low concentration).** The low concentration breakthrough tests were performed at 10 ppm  $H_2S$ . The details of the experimental procedure are described in

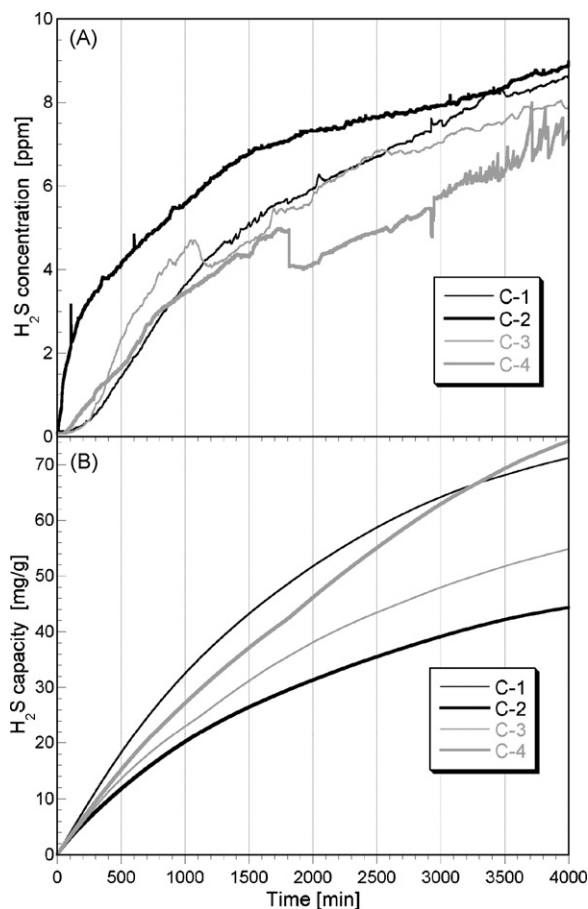


**Fig. 1.**  $H_2S$  breakthrough capacity curves at low concentration at 50% humidity (A) and the calculated changes in the capacity with the experimental time (B).

**Supplementary Information.** A relative humidity of 50% RH was used for the studies presented herein. Detection of the upstream and downstream contaminant concentration was monitored using electrochemical detector (Interscan Corp.; Chatsworth, CA; Model 117-LD). The sensor detection limit is 0.1 ppm of  $H_2S$ . Carbon samples were packed into a steel column (length 2.4 cm, internal diameter 3.8 cm, bed volume 28.9 cm<sup>3</sup>).  $H_2S$  was passed through the column of adsorbent at 30 L/min. The mean mesh size of the carbon particles is within  $12 \times 20$  [23]. The values of capacity reported at this paper are those measured at plateau of the capacity curves shown in Fig. 1(B). For the correlations, the reported values measured at arbitrary chosen  $C/C_0$  were used.

**2.2.5.2. Evaluation of  $H_2S$  sorption capacity (high concentration).** The dynamic test was used to evaluate the performance of the carbons for  $H_2S$  adsorption at high concentrations (3000 ppm). Carbon samples were packed into a glass column (length 370 mm, internal diameter 9 mm, bed volume 6 cm<sup>3</sup>).  $H_2S$  was passed through the column of adsorbent at 0.50 L/min. The details of the experimental procedure are described in [Supplementary Information](#). The samples were run with or without 2 h of pre-humidification with moist air (70% RH at 25 °C). A third sample of each activated carbon was run with a pre-drying step at 120 °C for 18 h followed by testing at dry condition with no pre-humidification step. As exhausted, they are referred to by adding to carbon name the following symbols -EP, -ED, and -D-ED, which represent the wet (pre-humidification and humid air), semi dry (as received and dry air), and dry conditions (pre-drying and dry air), respectively. As a breakthrough concentration, 100 ppm was arbitrarily chosen.

### 2.2.6. X-ray fluorescence (XRF) analysis

X-ray fluorescence (XRF) analysis was used to study the elemental content in carbons before and after H<sub>2</sub>S adsorption. The SPECTRO model 300T Benchtop Analyzer (ASOMA Instruments, Inc.) was used. The instrument has a titanium target X-ray tube and a high-resolution detector. A home-developed method scanning the emission energy range from 2 to 12 keV was applied.

### 2.2.7. Thermal analysis

**2.2.7.1. TGA–MS.** Thermo Gravimetric Analysis technique was used in combination with mass spectrometer (TGA–MS). A small amount of carbon sample was analyzed using a TA Instrument TGA 2950 Thermogravimetric Analyzer. The details of the experimental procedure are described in [Supplementary Information](#).

**2.2.7.2. Thermal desorption–gas chromatography–mass spectrometry method (TD/GC–MS).** A TDS-3 thermal desorption unit interfaced with an HP5890 GC (Gas Chromatograph) and an HP5972 MSD (mass selective detector) was used. Adsorbent tubes were conditioned at 300 °C for a minimum of 8 h. This conditioning procedure has proven to yield exceptionally clean blank runs of the adsorbent tubes. Calibration was achieved using a series of external standards. The details of the experimental procedure are described in [Supplementary Information](#).

## 3. Results and discussions

### 3.1. Impact of concentration and surface properties

H<sub>2</sub>S adsorption at low concentrations was measured and compared ([Fig. 1\(A\)](#)). Differences in the kinetics and capacity for H<sub>2</sub>S adsorption are seen based on the variations in the retention times and the shapes of the curves. Carbon C-4 has the longest breakthrough time for H<sub>2</sub>S removal while carbon C-2 has the shortest. The H<sub>2</sub>S removal capacity at low H<sub>2</sub>S concentration was calculated as a function of time using the breakthrough test conditions ([Fig. 1\(B\)](#)). Similar to the trend observed in the breakthrough curves, the H<sub>2</sub>S adsorption on carbon C-1 is initially slightly higher than that on carbon C-4 but with the progress of the test, the adsorption of H<sub>2</sub>S on C-4 carbon increases and it is higher than that on C-1 carbon. C-2 carbon has the lowest capacity for H<sub>2</sub>S among the four carbons studied.

One has to be aware that testing H<sub>2</sub>S adsorption at low concentrations requires more time and resources than that in accelerated conditions. Thus, most of the industry testing is usually run as accelerated, e.g. at high hydrogen sulfide concentrations. The results obtained in high concentration testing does not necessarily reflect the behavior of carbons at low concentrations [23,24]. Never-

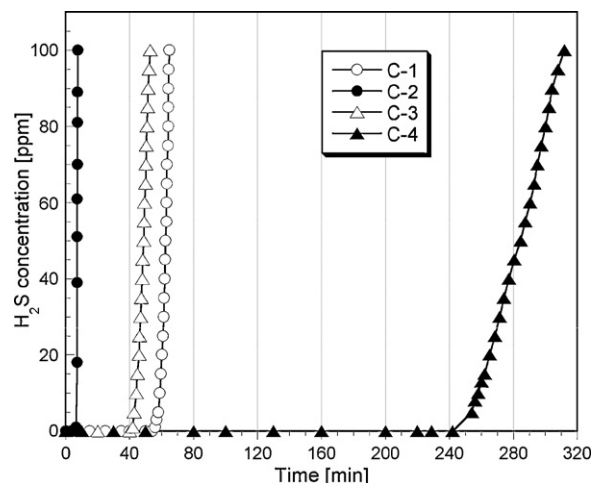


Fig. 2. H<sub>2</sub>S capacity curve at high concentration and 70% humidity.

theless, the trends indicated are certainly meaningful from the practical point of view. Since some discrepancies can be important for filtration, one of the objectives of this research is to focus on understanding them, if they exist. To compare the differences in the process of H<sub>2</sub>S retention on carbons as a result of variations in the concentration, breakthrough curves were also measured on the carbons at 3000 ppm of hydrogen sulfide. The measurements were first performed at 70% RH and 25 °C with pre-humidification of the carbon samples. The results are shown in [Fig. 2](#). Even though the order in the capacity values is the same as that for the low concentration measurements, carbon C-1 failed to match the performance of carbon C-4. The latter samples shows a significantly longer breakthrough time compared to the other carbons. The calculated capacities at low and high H<sub>2</sub>S concentrations are collected in [Table 1](#). A clear discrepancy in the H<sub>2</sub>S capacities between the low and high concentrations measurements is observed for all carbons which might be the result of the differences in the adsorption kinetics at both conditions. Although the H<sub>2</sub>S capacities for C-1, C-2 and C-3 carbons at low concentration exceeded their capacities at high concentration, the H<sub>2</sub>S capacities for the C-4 carbon showed opposite trend. The reverse behavior for carbon C-4 is most probably due to the presence of the oxidant chemical promoter on its surface. That promoter starts to contribute significantly at high H<sub>2</sub>S concentrations. These results, especially seen for C-2 carbon, demonstrate that kinetic limitations in accelerated test can lead to misinterpretation of the performance of filters exposed to very low H<sub>2</sub>S concentrations.

**Table 1**

H<sub>2</sub>S breakthrough capacity at low and high concentration, the amount of water pre-adsorbed and the surface pH values for carbon samples before and after H<sub>2</sub>S.

Sample	H <sub>2</sub> S breakthrough capacity		H <sub>2</sub> O adsorbed [mg/g]	Mass loss at 120 °C [%]	pH	
	At low [mg/g]	At high [mg/g]			In	Exh
C-1-EP	79.4	65.9	31.7	–	9.78	8.30
C-1-ED	–	15.5	–	–	9.78	9.73
C-1-D-ED	–	14.6	–	1.5	9.78	9.87
C-2-EP	45.1	5.7	88.4	–	7.14	6.83
C-2-ED	–	4.9	–	–	7.14	6.94
C-2-D-ED	–	4.2	–	1.2	7.14	6.38
C-3-EP	68.6	42.9	41.8	–	9.95	7.87
C-3-ED	–	30.9	–	–	9.95	7.87
C-3-D-ED	–	33.4	–	5.0	9.95	7.18
C-4-EP	91.1	215.4	77.6	–	9.70	2.80
C-4-ED	–	113.3	–	–	9.70	6.81
C-4-D-ED	–	79.3	–	8.3	9.70	7.92

**Table 2**

The parameters of the porous structure for the initial and exhausted carbons and the amount of acidic and basic species on their surfaces (for the initial samples).

Sample	$S_{\text{BET}}$ [m <sup>2</sup> /g]	$V_t$ [cm <sup>3</sup> /g]	$V_{\text{meso}}$ [cm <sup>3</sup> /g]	$V_{\text{mic}}$ [cm <sup>3</sup> /g]	$V_{\text{mic}}/V_t$	Acidic [mmol/g]	Basic [mmol/g]
C-1	1535	0.674	0.135	0.539	0.80	0.125	0.863
C-1-EP	1478	0.658	0.150	0.508	0.77		
C-1-ED	1599	0.713	0.170	0.543	0.76		
C-1-D-ED	1463	0.651	0.122	0.529	0.81		
C-2	877	0.378	0.022	0.356	0.94	0.251	0.381
C-3	1130	0.490	0.035	0.455	0.93	0.256	0.713
C-3-EP	1090	0.475	0.039	0.436	0.92		
C-3-ED	1061	0.459	0.031	0.428	0.93		
C-3-D-ED	1089	0.476	0.042	0.434	0.92		
C-4	931	0.401	0.023	0.378	0.94	0.150	1.096
C-4-EP	550	0.244	0.024	0.220	0.90		
C-4-ED	784	0.249	0.027	0.222	0.89		
C-4-D-ED	874	0.389	0.038	0.351	0.90		

It is important to mention that under the conditions of both experiments, the differences in flow rate at high and low concentrations might impact the residence time inside the column but are not expected to impact the mechanism by which H<sub>2</sub>S is adsorbed. The choice of going to lower flow rate with the higher concentration experiment was to allow the differentiation in the breakthrough curves between the various carbons due to the immediate breakthrough for carbons C-1, C-2 and C-3 at higher concentration and flow rate. The technical limitations also caused that different sensors were used at high and low concentration experiments.

To identify the influence of surface and chemical features of activated carbons on the capacity, surface chemistry and porosity were evaluated using Boehm titrations and sorption of nitrogen, respectively. The results are summarized in Table 2. Results from Boehm titrations indicate that carbons C-3 and C-2 have the highest amount of acidic groups on the surface whereas the amount of basic groups follow the order of C-4 > C-1 > C-3 > C-2. This trend is consistent with the observed trend in the breakthrough capacity. The surface pH values indicate that all carbons studied, except C-2, are basic. The parameters of porous structure show that carbon C-2 is the least microporous while carbon C-1 is the most microporous. The differences in the pore structures of the carbons are also seen in the pore size distributions presented in Fig. 3. All pores in C-2, C-3 and C-4 are smaller than 20 Å, whereas in the case of C-1, there is also a contribution of mesopores. The presence of small pores with a significant volume in the case of C-1 carbon can be the factor limiting the capacity at high concentrations of H<sub>2</sub>S. The kinetics at low concentration of H<sub>2</sub>S are more favorable and

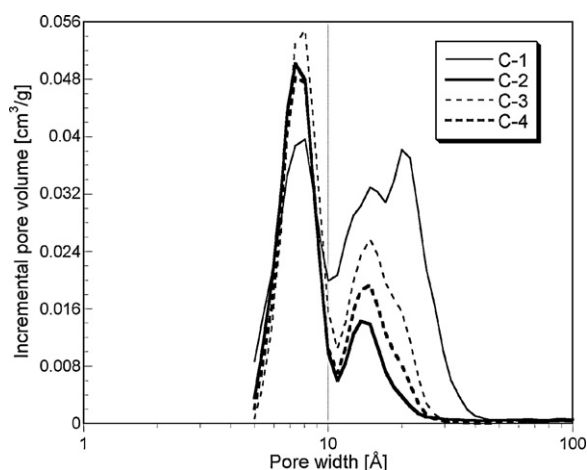


Fig. 3. Pore size distributions for the initial carbons.

H<sub>2</sub>S can accommodate in those small pores, similar in sizes to its molecule.

Understanding the relationship between the surface features of carbons and their affinity for H<sub>2</sub>S at low and high concentrations is very important to elucidate the adsorption mechanism of H<sub>2</sub>S. A correlation between the amount of H<sub>2</sub>S adsorbed at low concentrations and the amount of surface basic groups reveals the importance of basic groups for removing H<sub>2</sub>S at these conditions (Fig. 4(A)). Similar trend is also observed at high H<sub>2</sub>S concentrations for all carbons but C-4. The C-4 was excluded from the correla-

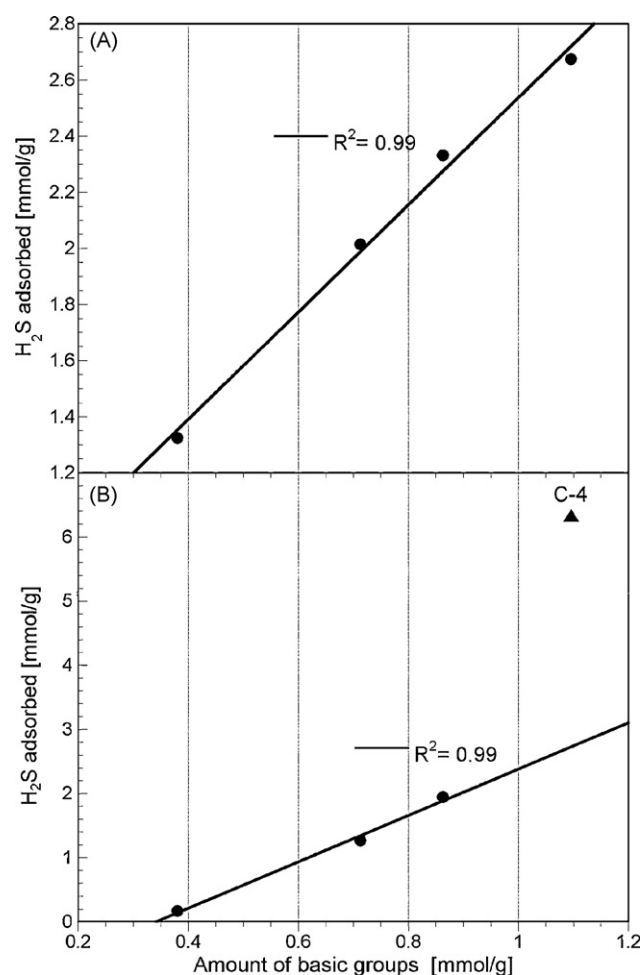


Fig. 4. Relationship between the amount of H<sub>2</sub>S adsorbed at low concentrations (A) and at high concentration (B) and the amount of basic groups.

tion because the noticeably higher amount of  $H_2S$  adsorbed on its surface suggests the catalytic role of a chemical promoter in enhancing the  $H_2S$  capacity. Although the structural parameters of the surface are known to play an important role in most physical adsorption processes, surface chemistry seems to be the predominant factor controlling the adsorption mechanism [9,10,12,16,25] since no correlation with the textural parameters could be established.

### 3.2. Impact of water

Besides an effect of the increase in the  $H_2S$  concentration in the challenge gas on the amount of hydrogen sulfide adsorbed on activated carbons, the presence of water on the surface or in the air stream is also expected to alter the performance of carbons [8,12,15,25]. As described in Section 2, the breakthrough measurements were also performed on all carbons using dry challenge gas and different surface moisture contents (e.g. pre-drying, pre-humidification). The results are summarized in Table 2. It is seen that carbons with the highest capacity under wet conditions (C-1 and C-4) are the most affected under dry conditions. The sample pre-drying has no clear impact on the  $H_2S$  removal except for carbon C-4 where the breakthrough time significantly decreased compared to the one without the pre-drying step. The presence of stored water on the surface impacts  $H_2S$  adsorption mainly for the carbon with a high capacity for  $H_2S$  under humid conditions. It is known that water on the surface of carbons, even in small quantities, enhances their performance as  $H_2S$  adsorbents [12,16,25]. It happens mainly when  $H_2S$  is adsorbed via a reactive adsorption mechanism, which involves oxidation [8,9,12,25,26]. The role of surface chemistry and a chemical promoter is very important in such situations. Since carbon C-4 is impregnated with both alkaline and oxidant promoters, the impact of water on its performance can follow the mechanism proposed by Bandoz and coworkers where an alkaline surface enhances the conversion of  $H_2S$  to  $HS^-$  ions in the film of water and those ions are oxidized to sulfur oxides. It is interesting that under very dry conditions (with sample pre-drying), carbon C-4 still outperforms all the other carbons even when they are tested at high humid conditions. This can be the result of the high affinity of C-4 to attract  $H_2S$  due to the presence of the alkaline impregnant on its surface.

In Table 1 the mass loss as a result of drying of the carbon samples prior to the breakthrough testing are also collected along with the surface pH values of carbons before and after  $H_2S$  adsorption. As discussed above, carbon C-4 has the highest  $H_2S$  capacity under wet conditions while carbon C-2 has the lowest. The effect of various water levels on the performance is most visible for C-4 and C-1. Pre-drying the carbons at  $120^\circ C$  followed by the breakthrough measurements at dry conditions has no clear impact on the  $H_2S$  capacity except for carbon C-4 where the capacity significantly decreased in comparison to the tests conducted with no pre-drying. The fact that under these severe dry conditions, the capacity of carbon C-4 for  $H_2S$  is still much higher than those of all other carbons under all experimental conditions evaluated in this study, lead us to conclude that the elevated amount of basic species, not necessarily the surface groups as assumed in Boehm titration, will lead to enhanced  $H_2S$  removal capacity.

The affinity of carbons to attract water was tested by measuring the water adsorption isotherms (Fig. 5). The results indicate that C-4 is the most hydrophilic and C-1 is the most hydrophobic carbon. However, at 70% humidity all carbons but C-1 adsorb similar amounts of water. This might be caused by the polarity of the surface functional groups, polarity of the impregnants and also the presence of inorganic matter. The latter should not affect sig-

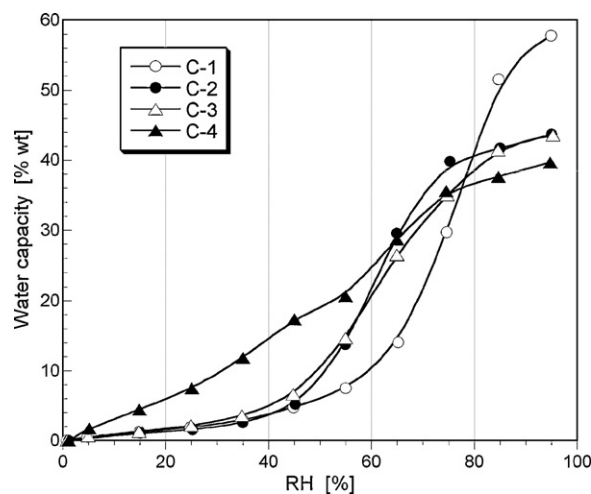


Fig. 5. Water isotherms for carbons C-1, C-2, C-3 and C-4.

nificantly the water adsorption behavior since the content of ash in the carbons tested varies from 1.9% to 3.2%, which is typical to coconut-shell-based carbons. The mentioned above differences in surface hydrophilicity can also play a role in the differences in the kinetics of adsorption on C-1 carbon at low and high concentrations of hydrogen sulfide.

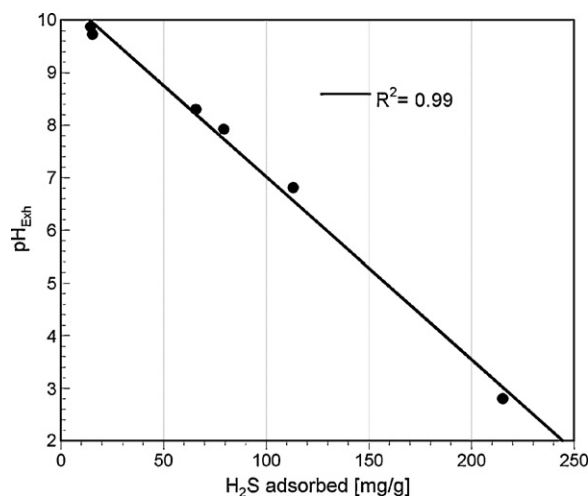
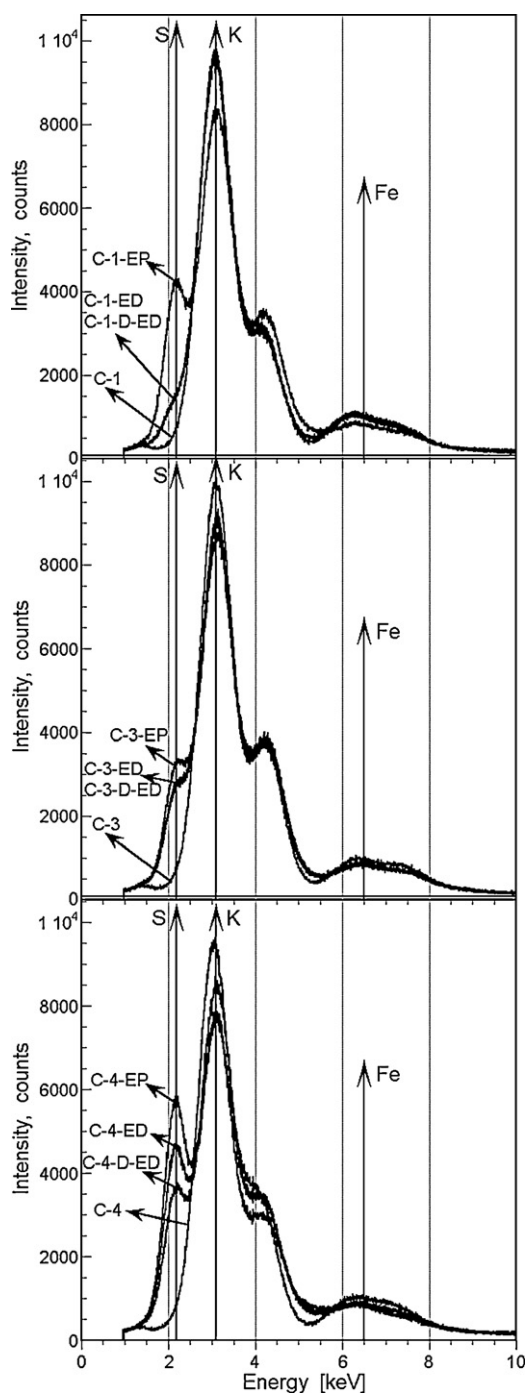


Fig. 6. Relationship between the surface pH after  $H_2S$  adsorbed and the amount of  $H_2S$  adsorbed on C-4 and C-1 carbons.

Table 3

Mass loss at different temperature ranges and the amount of sulfur from breakthrough capacity at high concentration of  $H_2S$ .

Sample	Mass loss [%]				$S_{H_2S}$ [wt%]
	>200 °C	200–350 °C	350–550 °C	550–800 °C	
C-1	3.36	0.70	1.49	2.22	
C-1-EP	5.51	1.09	1.97	2.41	6.2
C-1-ED	2.02	0.71	0.76	2.36	1.5
C-1-D-ED	2.02	0.56	0.85	2.75	1.4
C-3	7.22	1.07	1.21	2.23	
C-3-EP	9.82	1.79	1.91	2.63	4.0
C-3-ED	3.21	1.87	1.71	2.85	2.9
C-3-D-ED	2.80	1.32	1.42	2.43	3.1
C-4	9.29	0.97	1.57	2.68	
C-4-EP	12.62	3.53	7.02	3.57	20.3
C-4-ED	2.47	2.54	6.63	3.54	10.7
C-4-D-ED	2.34	1.81	3.54	3.86	7.5



**Fig. 7.** X-ray fluorescence spectra for carbons C-1, C-3 and C-4 before and after H<sub>2</sub>S adsorption at various conditions.

The changes in the surface chemistry after H<sub>2</sub>S adsorption at high concentrations are reflected in the pH values of the surface, which decreased for all carbons after H<sub>2</sub>S adsorption under all test conditions (Table 1). This change is the most pronounced under wet conditions and for carbon C-4. Its surface became very acidic (pH=2.8) which suggests formation of strong oxy-sulfur acids [16,26]. Also the basic groups disappeared from the surface of this carbon as a result of reaction/neutralization with H<sub>2</sub>S and its reactive adsorption. To consider the mechanism of adsorption, it is important to have a fundamental understanding of the changes within the system. It is important to mention

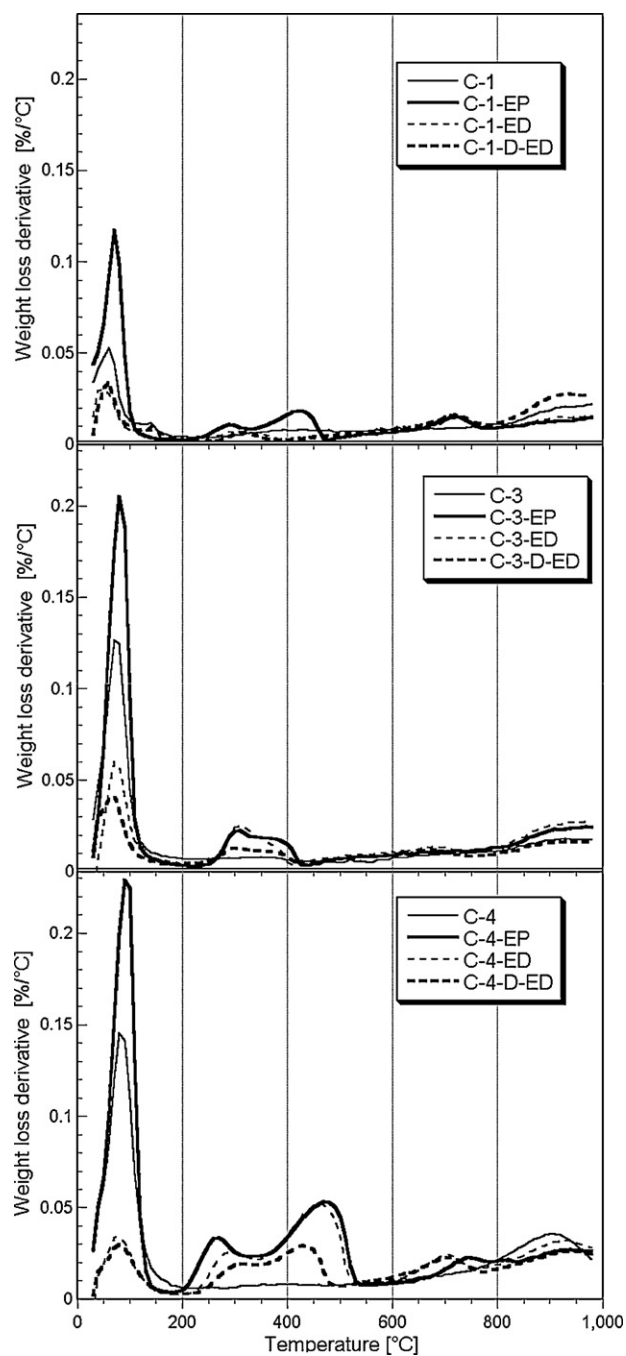


**Fig. 8.** DTG curves showing the changes in the weight loss with temperature after H<sub>2</sub>S adsorption at high H<sub>2</sub>S concentration and different humidity conditions.

that the pH values of the surface of exhausted C-4 and C-1 carbons directly correlate with the amount of H<sub>2</sub>S adsorbed (Fig. 6). This indicates that there are similarities in the reactive adsorption mechanism between those two carbons. The results for C-2 and C-3 carbons were not analyzed due to their low H<sub>2</sub>S capacities and thus small differences in the surface chemistry before and after adsorption.

### 3.3. Characterization of the reactive adsorption products

The effect of H<sub>2</sub>S exposure on the changes in the sulfur content of the activated carbons was studied using X-ray fluorescence

**Table 4**  
The types and amounts of the sulfur compounds desorbed at 250 °C (from TD–GC–MS analysis).

	Sulfur (S8) [μg/g]	Sulfur dioxide (μg/g)	Carbon disulfide (μg/g)	Thiophene (μg/g)	Total sulfur (μg/g)
C-1	–	–	–	–	–
C-1-EP	–	1.49	–	–	1.49
C-1-ED	–	0.48	0.22	–	0.71
C-1-D-ED	–	1.08	0.58	0.05	1.71
C-3	–	–	–	–	–
C-3-EP	–	2.19	3.27	–	5.46
C-3-ED	–	1.38	–	–	1.38
C-3-D-ED	–	1.85	–	–	1.87
C-4	–	–	–	–	–
C-4-EP	1.41	0.12	–	–	1.53
C-4-ED	10.76	–	–	–	10.76
C-4-D-ED	2.68	–	–	0.06	2.74

and thermal analysis. The XRF spectra are presented in Fig. 7. Since the capacity on C-2 was very small, the samples were not analyzed for sulfur. An increase in the sulfur content upon adsorption is noticed and the intensity of the peak is a function of the amount of water present during H<sub>2</sub>S adsorption. From the point of view of potassium and iron content, the similar spectra are found for the initial carbons. High content of potassium is characteristic for coconut-shell-based carbons [27]. This element increases their surface basicity.

Thermal analysis was performed immediately after H<sub>2</sub>S adsorption at high concentrations on all carbons except for C-2, which has a negligible capacity for H<sub>2</sub>S. These results were compared to those on the same carbon, which was not exposed to H<sub>2</sub>S. The differential thermal gravimetric (DTG) curves (Fig. 8), show the appearance of several new peaks after H<sub>2</sub>S adsorption. They represent the weight losses due to desorption of water, H<sub>2</sub>S and/or its adsorption products. The weight loss below 200 °C is mainly related to the desorption of water and weakly adsorbed H<sub>2</sub>S and SO<sub>2</sub> [25,26]. The intensity of this peak increased for all carbons tested under humid conditions. The higher temperature DTG peaks are assigned to the removal of the products of surface reactions or thermal decomposition of those products. The peak between 200 °C and 350 °C represents the removal of SO<sub>2</sub> from the decomposition of oxysulfur acids [12,16] or H<sub>2</sub>S from decomposition of alkali metal sulfides, while the peak at 350 °C–600 °C is probably the result of the desorption of elemental sulfur and decomposition of the surface reaction products [25,26]. The intensities of the second and third peaks on the DTG curves increase with an increase the amount of water on the surface. This is in agreement with the increase in the amount of H<sub>2</sub>S adsorbed and likely with an increase in the extent of polysulfides formations [12,16,25,26]. A more detailed quantitative evaluation for the TA data is presented in Table 3. The mass losses on carbons at different temperature intervals were calculated for all samples before and after H<sub>2</sub>S adsorption. That mass loss is higher under wet conditions than under dry ones due to the oxidation of sulfur and involvement of water.

Although the breakthrough curves along with the DTG and XRF curves provided semi-qualitative analysis of the surface changes resulted from H<sub>2</sub>S adsorption, the data offer no direct information on the type of species desorbed and the mechanism of their adsorption. Thus TD/GC–MS analysis was performed on the carbons before and after H<sub>2</sub>S adsorption at high concentrations under all experimental conditions. The results summarized in Table 4 show the presence of different forms of sulfur compounds on the surface of the carbon samples after H<sub>2</sub>S adsorption. Species such as octa-sulfur, sulfur dioxide, carbon disulfide, and thiophene are detected. One has to be aware that this analysis was done only on the off-gases released from the surface up to 250 °C so the

majority of surface reaction products released at temperatures higher than 250 °C are not analyzed. Thus the total amount of sulfur calculated from the TD/GC–MS analysis is much lower than the ones calculated from the breakthrough curves and thermal analysis.

The speciation of the sulfur compounds using TD/GC–MS provided interesting information but due to the experimental limitations, the results are not comprehensive. For a more detailed qualitative analysis, the C-4 samples were then analyzed using TGA–MS analysis. DTG curves along with ion current curves for all samples are shown in Fig. 9. The curves follow a similar trend to those presented in Fig. 8. By tracking the mass spectrometer ion current for the ions of *m/z* ratio of 18–96, the ions of *m/z* equal to 18, 33, 34, 48, 64 and 66 were detected as shown in Fig. 9(B), (C), (D), (E), (F) and (G). It is interesting to note the similarity in the ion current profile for the ions of *m/z*=33 and 34. The ion current profile for the ions of *m/z*=48, 64 and 66 are also similar. The *m/z*=33 most probably represents the ion HS<sup>−</sup> which is one of the H<sub>2</sub>S reactive adsorption product or can be the result the fragmentation of hydrogen sulfide or dihydrogen disulfide after thermal decomposition of sulfides. Fragments with *m/z*=48 and 66 might be related to SO and SO<sub>2</sub>, respectively. It is interesting that some H<sub>2</sub>S desorbs in the temperature range 350–550 °C and is represented by the presence of ions of *m/z*=33 and 34. That H<sub>2</sub>S can be the result of the reduction of SO<sub>2</sub>/SO<sub>3</sub> from decomposition of oxyacids by carbon at that high temperature and decomposition of polysulfides. We do not expect that physically adsorbed H<sub>2</sub>S desorbs at these conditions [25,26]. HS–SH desorbs between 250 and 550 °C which is supported by the presence of ions of *m/z*=66, 64 and 33. Sulfur oxides most probably are the oxidation products of the reaction between the various forms of sulfur compounds present of the surface and the oxygen gas and the oxidizer. Their sources are in HS<sup>−</sup>, H<sub>2</sub>S, elemental sulfur and polysulfides as shown in the TD/GC–MS and TGA–MS results. Formation of sulfur oxides and H<sub>2</sub>SO<sub>4</sub> is supported by the significant decrease in the surface pH for C-4, mainly under wet conditions. Although some oxides of sulfur can be formed during the TD–MS experiment since traces of O<sub>2</sub> gas can be present either in nitrogen (UHP) or chemisorbed on the surface, their quantity should be very small. The presence of sulfur oxyacids is supported by the ion current curve for *m/z*=18 which shows water desorption profile in the same temperature range as those for *m/z*=48, 64 and 66 curves.

In brief, the presence of various forms of sulfur compounds in addition to the oxides of sulfur on the surface of carbon C-4 after H<sub>2</sub>S adsorption at the different humidity levels indicates that the chemical reactions are involved in H<sub>2</sub>S retention. The alkaline and chemical promoter present on the surface and water facilitate dissociation, dimerization and oxidation reactions [8,10,12,13,16,25]. Increasing the pH of the carbon surface through impregnation with

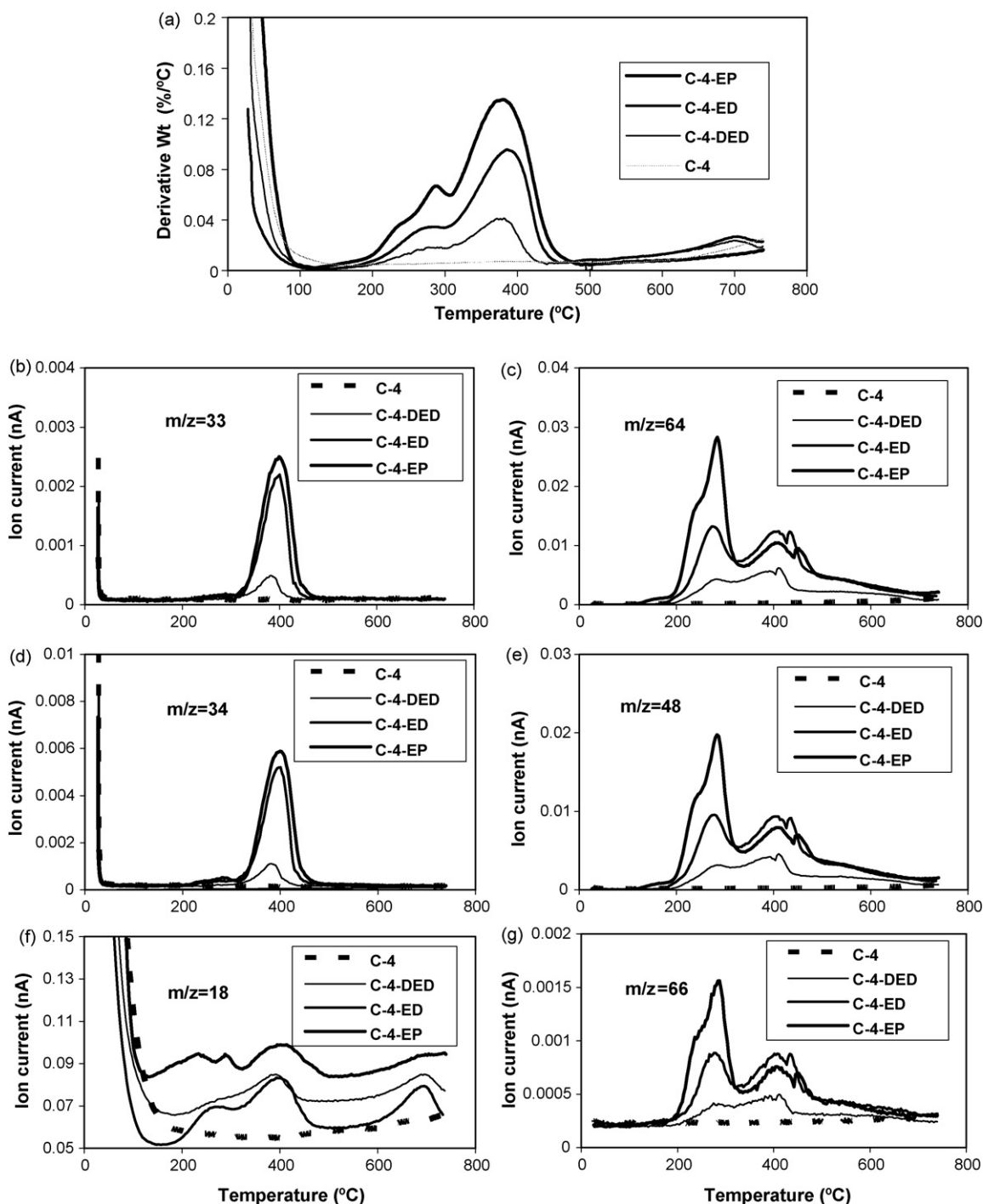


**Fig. 9.** DTG curves (A) for all carbon C-4 samples before and after H<sub>2</sub>S adsorption at various conditions and their mass spectrometer ion current curves for the ions of  $m/z = 33$ , 64, 34, 48, 18, and 66 (B, C, D, E, F, and G, respectively).

the base increases the surface affinity to specifically attract H<sub>2</sub>S. Then the oxidizer contributes to the formation of polysulfides, hydrogen disulfide and oxides of sulfur.

Adsorption of H<sub>2</sub>S and its surface reaction products is expected to be accompanied by a change in the structural features of the carbon due the deposition of those compounds in the pore space. To evaluate such changes after H<sub>2</sub>S adsorption under dry and wet conditions, characterization of the pore structure was done on all carbons exposed to high concentration of H<sub>2</sub>S (Table 2). Exam-

ples of the changes in PSD for carbon C-4 before and after H<sub>2</sub>S adsorption are presented in Fig. 10. After H<sub>2</sub>S adsorption under dry and humid conditions, the PSD curves show a decrease in the volume of pores of all sizes. The most pronounced effects are seen after pre-humidification where about 20 wt% of sulfur was retained on the surface. The same trends are observed for all other carbons for which the volumes of micropores and surface areas decrease as a result of deposition of sulfur containing species (Table 2).



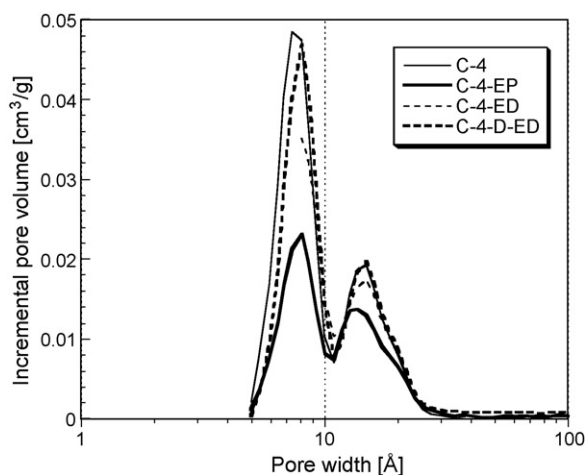


Fig. 10. Pore size distribution for carbon C-4 before and after H<sub>2</sub>S adsorption at high H<sub>2</sub>S concentrations.

#### 4. Conclusions

H<sub>2</sub>S breakthrough curves were measured on various coconut-shell-based carbons having different surface chemical and textural features. The shapes of the breakthrough curves differ at high and low concentration of H<sub>2</sub>S, which can be related to the kinetics of surface reactions. They seem to visibly affect the removal process. The amount of H<sub>2</sub>S adsorbed at both concentrations showed a clear dependence on the amount of basic groups present on the surface. Moisture in the challenge gas and water on the surface proved to be important factors enhancing H<sub>2</sub>S removal. Water on the activated carbon surface, even in very small quantity, significantly increased the amount of H<sub>2</sub>S adsorbed when the breakthrough testing was carried out in the absence of moisture in the challenge gas. Water contributes to the adsorption process via its involvement in the dissociation of H<sub>2</sub>S and its further oxidation to sulfur oxides. The presence of a chemical promoter, classified as an oxidant, on the carbon surface clearly increased its H<sub>2</sub>S adsorption capacity compared to the other carbons, especially in the presence of water. This modified carbon showed higher capacity at both high and low H<sub>2</sub>S concentrations even at very dry conditions. The main forms of sulfur compounds thermally desorbed from the exhausted carbon surface were elemental sulfur, sulfur oxides, carbon sulfide, polysulfides and hydrogen sulfide. The latter is likely the results of the decomposition of polysulfides and reduction of sulfur oxides, which are the important products of surface reactions. The variety of products proves the complexity of reactive adsorption of H<sub>2</sub>S on alkaline activated carbons.

#### Acknowledgments

The authors are grateful to Ms. Patricia Libra for her help in performing the TGA–MS analysis and to Mr. Dave Mulder for reviewing the paper.

#### Appendix A. Supplementary data

Supplementary data associated with this article can be found, in the online version, at [doi:10.1016/j.cej.2009.08.010](https://doi.org/10.1016/j.cej.2009.08.010).

#### References

- [1] P. Forzatti, L. Lietti, Catalyst deactivation, *Catal. Today* 52 (1999) 165–181.
- [2] Y. Xiao, Sh. Wang, D. Wu, Q. Yuan, Catalytic oxidation of hydrogen sulfide over unmodified and impregnated activated carbon, *Sep. Purif. Technol.* 59 (2008) 326–332.
- [3] W.J. Powers-Schilling, Olfaction: chemical and psychological considerations, in: *Proc. of Nuisance Concerns in Animal Management: Odor and Flies Conference*, Gainesville, Florida, 1995.
- [4] H. Duan, R. Yan, L.C. Koe, X. Wang, Combined effect of adsorption and biodegradation of biological activated carbon on H<sub>2</sub>S biotrickling filtration, *Chemosphere* 66 (2007) 1684–1691.
- [5] D. Gabriel, M.A. Deshusses, Retrofitting existing chemical scrubbers to biotrickling filters for H<sub>2</sub>S emission control, *Proc. Natl. Acad. Sci. U.S.A.* 100 (2003) 6308–6312.
- [6] D. Gabriel, M.A. Deshusses, Performance of a full-scale biotrickling filter treating H<sub>2</sub>S at a gas contact time of 1.6 to 2.2 seconds, *Environ. Prog.* 22 (2003) 111–118.
- [7] E. Smet, P. Lens, H. van Langenhove, Treatment of waste gases contaminated with odorous sulfur compounds, *Crit. Rev. Environ. Sci. Technol.* 28 (1998) 89–117.
- [8] M. Seredych, T.J. Bandoz, Role of microporosity and nitrogen functionality on the surface of activated carbon in the process of desulfurization of digester gas, *J. Phys. Chem. C* 112 (2008) 4704–4711.
- [9] A. Bagreev, M.J. Angel, I. Dukhno, Y. Tarasenko, T.J. Bandoz, Bituminous coal-based activated carbons modified with nitrogen as adsorbents of hydrogen sulfide, *Carbon* 42 (2004) 469–476.
- [10] R. Yan, D.T. Liang, L. Tsen, J.H. Tay, Kinetics and mechanisms of H<sub>2</sub>S adsorption by alkaline activated carbon, *Environ. Sci. Technol.* 36 (2002) 4460–4466.
- [11] W. Feng, S. Kwon, E. Borguet, R. Vidic, Adsorption of hydrogen sulfide onto activated carbon fibers: effect of pore structure and surface chemistry, *Environ. Sci. Technol.* 39 (2005) 9744–9749.
- [12] A. Bagreev, T.J. Bandoz, On the mechanism of hydrogen sulfide removal from moist air on catalytic carbonaceous adsorbents, *Ind. Eng. Chem. Res.* 44 (2005) 530–538.
- [13] R. Yan, T. Chin, Y.L. Ng, H. Duan, D.T. Liang, J.H. Tay, Influence of surface properties on the mechanism of H<sub>2</sub>S removal by alkaline activated carbons, *Environ. Sci. Technol.* 38 (2004) 316–323.
- [14] J. Guo, Y. Luo, A.Ch. Lua, R.-A. Chi, Y.-L. Chen, X.-T. Bao, Sh.-X. Xiang, Adsorption of hydrogen sulphide (H<sub>2</sub>S) by activated carbons derived from oil-palm shell, *Carbon* 45 (2007) 330–336.
- [15] S. Bashkova, F.S. Baker, X. Wu, T.R. Armstrong, V. Schwartz, Activated carbon catalyst for selective oxidation of hydrogen sulphide: on the influence of pore structure, surface characteristics, and catalytically-active nitrogen, *Carbon* 45 (2007) 1354–1363.
- [16] A. Bagreev, T.J. Bandoz, A role of sodium hydroxide in the process of hydrogen sulfide adsorption/oxidation on caustic-impregnated activated carbons, *Ind. Eng. Chem. Res.* 41 (2002) 672–679.
- [17] L.M. Leuch, A. Subrenat, P. Le Cloirec, Hydrogen sulfide adsorption and oxidation onto activated carbon cloths: applications to odorous gaseous emission treatments, *Langmuir* 19 (2003) 10869–10877.
- [18] L. Meljac, L. Perier-Camby, G. Thomas, Creation of active sites by impregnation of carbon fibers: application to the fixation of hydrogen sulfide, *J. Coll. Inter. Sci.* 274 (2004) 133–141.
- [19] H.P. Boehm, Chemical identification of surface groups, in: *Advances in Catalysis*, Academic Press, New York, 1966, pp. 179–274.
- [20] H.P. Boehm, Some aspects of the surface chemistry of carbon blacks and other carbons, *Carbon* 32 (1994) 759–769.
- [21] J.P. Olivier, Modeling physical adsorption on porous and nonporous solids using density functional theory, *J. Por. Mater.* 2 (1995) 9–17.
- [22] C.M. Lastoskie, K.E. Gubbins, N.J. Quirk, Pore size distribution analysis of microporous carbons: a density functional theory approach, *J. Phys. Chem.* 97 (1993) 4786–4796.
- [23] Y. Elsayed, P. Lodewyckx, J. Exley, A. Dallas, Filter life estimation methods applied at low organic contaminant concentrations, in: *Carbon Conference*, Seattle, 2007.
- [24] A. Bagreev, S. Katikaneni, S. Parab, T.J. Bandoz, Desulfurization of digester gas: prediction of activated carbon bed performance at low concentrations of hydrogen sulfide, *Catal. Today* 99 (2005) 329–337.
- [25] T.J. Bandoz, Desulfurization on activated carbons, in: T.J. Bandoz (Ed.), *Activated Carbon Surfaces in Environmental Remediation*, Elsevier, Oxford, 2006, pp. 213–292.
- [26] T.J. Bandoz, On the adsorption/oxidation of hydrogen sulfide on activated carbons at ambient temperatures, *J. Coll. Inter. Sci.* 246 (2002) 1–20.
- [27] M.M. van der Merwe, T.J. Bandoz, A study of ignition of metal impregnated carbons: the influence of oxygen content in the activated carbon matrix, *J. Coll. Inter. Sci.* 282 (2005) 102–108.